Environment International 137 (2020) 105530

Contents lists available at ScienceDirect

Environment International

journal homepage: www.elsevier.com/locate/envint

Induction and recovery of CpG site specific methylation changes in human bronchial cells after long-term exposure to carbon nanotubes and asbestos

Deniz Öner[a,1], Manosij Ghosh[a,1], Robin Coorens[a], Hannelore Bové[b], Matthieu Moisse[c], Diether Lambrechts[c,d], Marcel Ameloot[b], Lode Godderis[a,e], Peter H.M. Hoet[a,*]

[a] KU Leuven, Department of Public Health and Primary Care, Unit of Environment and Health, Laboratory of Toxicology, 3000 Leuven, Belgium
[b] Hasselt University, Biomedical Research Institute, Agoralaan Building C, 3590 Diepenbeek, Belgium
[c] KU Leuven, Department of Human Genetics, Laboratory for Translational Genetics, 3000 Leuven, Belgium
[d] VIB, VIB Center for Cancer Biology, Laboratory for Translational Genetics, 3000 Leuven, Belgium
[e] Idewe, External Service for Prevention and Protection at Work, B-3001 Leuven, Belgium

ARTICLE INFO

Handling Editor: Yong-Guan Zhu

Keywords:
Carbon nanotube
Asbestos
Epigenetics
DNA methylation

ABSTRACT

Introduction: Inhalation of asbestos induces lung cancer via different cellular mechanisms. Together with the increased production of carbon nanotubes (CNTs) grows the concern about adverse effects on the lungs given the similarities with asbestos. While it has been established that CNT and asbestos induce epigenetic alterations, it is currently not known whether alterations at epigenetic level remain stable after withdrawal of the exposure. Identification of DNA methylation changes after a low dose of CNT and asbestos exposure and recovery can be useful to determine the fibre/particle toxicity and adverse outcome.

Methods: Human bronchial epithelial cells (16HBE) were treated with a low and non-cytotoxic dose (0.25 μg/ml) of multi-walled carbon nanotubes (MWCNTs-NM400) or single-walled carbon nanotubes (SWCNTs-SRM2483) and 0.05 μg/ml amosite (brown) asbestos for the course of four weeks (sub-chronic exposure). After this treatment, the cells were further incubated (without particle/fibre) for two weeks, allowing recovery from the exposure (recovery period). Nuclear depositions of the CNTs were assessed using femtosecond pulsed laser microscopy in a label-free manner. DNA methylation alterations were analysed using microarrays that assess more than 850 thousand CpG sites in the whole genome.

Results: At non-cytotoxic doses, CNTs were noted to be incorporated with in the nucleus after a four weeks period. Exposure to MWCNTs induced a single hypomethylation at a CpG site and gene promoter region. No change in DNA methylation was observed after the recovery period for MWCNTs. Exposure to SWCNTs or amosite induced hypermethylation at CpG sites after sub-chronic exposure which may involve in 'transcription factor activity' and 'sequence-specific DNA binding' gene ontologies. After the recovery period, hypermethylation and hypomethylation were noted for both SWCNTs and amosite. Hippocalcinlike 1 (*HPCAL1)*, protease serine 3 (*PRSS3),* kallikrein-related peptidase 3 *(KLK3)*, kruppel like factor 3 (*KLF3)* genes were hypermethylated at different time points in either SWCNT-exposed or amosite-exposed cells.

Conclusion: These results suggest that the specific SWCNT (SRM2483) and amosite fibres studied induce hypo- or hypermethylation on CpG sites in DNA after very low-dose exposure and recovery period. This effect was not seen for the studied MWCNT (NM400).

1. Introduction

Current understanding of carbon nanotubes (CNT) toxicity suggests that some CNTs are more toxic than others. Some multi-walled carbon nanotubes (MWCNTs) induced genotoxicity *in vitro* and adverse effects in the lung, whereas carcinogenic risk remained elusive for some types (Muller et al., 2009). Exposure to MWCNT-7 (Mitsui) has been associated with carcinogenesis and asbestos-like pathogenesis in the mesothelial linings of the rodents (Kasai et al., 2015; Poland et al., 2008; Sargent et al., 2014), which lead to the classification of MWCNT-7 as possibly carcinogenic to humans (Group 2B) by International Agency for Research on Cancer (IARC Monographs 111; 2014). Other forms of

* Corresponding author.
E-mail address: peter.hoet@kuleuven.be (P.H.M. Hoet).
[1] Deniz Öner and Manosij Ghosh have contributed equally.

https://doi.org/10.1016/j.envint.2020.105530
Received 3 July 2019; Received in revised form 21 January 2020; Accepted 25 January 2020
Available online 18 February 2020
0160-4120/ © 2020 The Authors. Published by Elsevier Ltd. This is an open access article under the CC BY-NC-ND license (http://creativecommons.org/licenses/BY-NC-ND/4.0/).

MWCNTs and single-walled carbon nanotubes (SWCNTs) are not classifiable as to their carcinogenicity to humans (Group 3). Exposure to SWCNTs has been associated with disruption at mitotic spindles, cytotoxicity, genotoxicity and increased fibrosis (Kisin et al., 2007; Sargent et al., 2012; Shvedova et al., 2008), however, no carcinogenicity has been reported for exposure to SWCNTs in rodents so far. Additionally, there are growing concerns regarding CNT-asbestos analogy.

The most important physicochemical similarities between asbestos and CNTs are their fibre shape (and high aspect ratio), insolubility, biopersistency and the potential presence of transition metals (Donaldson et al., 2013; Hoet et al., 2004). On the other hand, the surface of CNTs is a hexagonal structure and the diameter of CNTs is in the nano range. For SWCNTs, the diameter is smaller than 2 nm and for MWNCTs larger than 10 nm – resulting in a larger surface area and reactivity, in comparison to asbestos fibres. Furthermore, CNTs can be engineered in different forms and therefore, toxicity may differ between different types of CNT fibres. This is particularly important for safety measures during CNT-production and handling.

Inhalation of asbestos fibres, either in occupational or environmental settings, is associated with an increase in neoplastic diseases such as bronchogenic carcinoma (i.e. adenocarcinoma and mesothelioma) (Norbet et al., 2015). Typically, asbestos-induced diseases show a long latency period between the first exposure and the disease diagnosis, posed mostly years after the exposure has ceased. For instance, among the insulation workers who were exposed to asbestos fibres, lung cancer diagnosis peaked 30–35 years later (Selikoff et al., 1980). Studies show that fibres, that are physicochemically similar to asbestos, can induce the same pathological consequences in the lung, as illustrated for example by effects observed in relation to environmental exposure to zeolite (erionite) (Emri et al., 2002). Studies have now indicated that the toxicity of carbon nanotubes (CNTs), either as multi-walled (MWCNT) or single-walled (SWCNT), are accentuated by their high aspect ratio, stiffness, tensile strength and biopersistance similar to asbestos (Alshehri et al., 2016; Boyles et al., 2015; Bussy et al., 2012; Donaldson et al., 2013, 2010; Murphy et al., 2011; Poulsen et al., 2016).

While cyto-genotoxic and genomic changes are clearly associated with CNT and asbestos induced disease phenotype, emerging evidences suggest that molecular changes important in high aspect fibres toxicity may involve epigenetic alterations. Investigations regarding the alterations caused by occupational and environmental exposures to asbestos reveal aberrant epigenetic changes (Christensen et al., 2009, 2008). Asbestos (crocidolite and chrysotile) induced changes in DNA methylation has reported in MeT5A cells (Casalone et al., 2018) associated with “cell adhesion”. For asbestos exposure (amosite, crocidolite and chrysotile) in 16HBE cells (Emerce et al., 2019; Öner et al., 2018b), we also observed gene specific DNA methylation alteration involved in the regulation of Rho-protein signal transduction, homeobox genes, ATP-binding and WNT-group of genes. Some of the differentially methylated regions observed in these invitro studies have also been identified in lung cancer tissue from asbestos exposed patients (Gulino et al., 2016). Since epigenetic deregulation is emerging as a key feature of lung cancer, more specifically for asbestos; in recent years, we have designed series of studies to understand the effect of CNT and asbestos on DNA methylation. Our studies in THP-1 cells (Öner et al., 2017), and in rodent model (Tabish et al., 2017), and a small group of MWCNT exposed workers (Ghosh et al., 2017), we have observed gene promoter-specific hypo and hypermethylation; involved in several signalling cascade pathways, vascular endothelial growth factor and platelet activation pathways.

For both asbestos and carbon nanotubes (Chen et al., 2014; Duke and Bonner, 2018; Gulino et al., 2016; Kamp, 2009; Khalil et al., 1996; Polimeni et al., 2016) epithelial to mesenchymal transition is a key step and has been associated with pulmonary fibrosis. To understand the mechanism involved, we have extensively studied the epigenetic and transcriptomics changes in bronchial epithelial cell (Emerce et al., 2019; Ghosh et al., 2018; Öner et al., 2018a, 2018b). We found that aberrations in gene promoter hypomethylation occurs after acute exposure to MWCNTs and CpG site hypermethylation or hypomethylation occurs after acute exposure to SWCNTs in human bronchial cells (16HBE) cells (Ghosh et al., 2018; Öner et al., 2018a). These epigenetic alterations were associated with transcriptomic changes linked to WNT and TGF-β signalling pathways and fibroblast proliferation. However, like in most *in vitro* studies, our study design had limitations in imitating real-life exposure, mostly because of the high concentration tested and short duration (24 h) of exposure.

Occupational exposure to particles and fibres such as asbestos are known to occur continuously during the course of employment (> 20 years) and stops with the end of employment, however disease appears much later in life. In most cases real-life exposure levels are much lower than normally tested *in vitro* and occur continuously for a longer period. When small numbers of fibres reach the lungs, they may leave epigenetic marks at the genome. It is currently not known whether such epigenetic alterations remain even after the exposure stops, leading to a risk of disease in future years. Although in this study we do not directly look at the association between epigenetic alteration induced by high ration fibres and disease, it can be hypothesized that DNA methylation may act as an intermediate step towards disease development and is highly dynamic during exposure and after cessation. To address some of these issues, in this study, we performed a long-term and low-dose asbestos- and CNT-exposure in 16HBE cells, as a better imitation of real-life sub-chronic exposure on lung bronchial epithelial cells. In addition, we added two weeks of recovery period in order to investigate whether epigenetically modified CpG sites were persistent/recovering over the multiple cell divisions.

2. Materials and method

2.1. Materials

The Union for International Cancer Control (UICC) reference amosite (South African) was purchased from SPI Supplies (Structure Probe Inc., West Chester, USA). The preparation of the asbestos samples was published previously (Timbrell and Rendall, 1972). Two types of reference CNTs were used: MWCNTs and SWCNTs. MWCNT-NM400, were purchased from Joint Research Center (JRC, Ispra, Italy) (Rasmussen et al., 2013). SWCNT-SRM2483, were purchased from National Institute of Science and Technology (NIST, Maryland, USA). Producers have extensively performed characterization of the materials. Additional characterizations (i.e. TEM, DLS and endotoxin measurements) were investigated in our previous studies (Ghosh et al., 2018; Öner et al., 2018a, 2017). In brief, MWCNTs have a diameter about 11 nm and SWCNTs have a diameter about 0.8 nm. MWCNTs are smaller than 1 μm in length whereas pristine SWCNTs are approximately 8 μm. Both CNTs have high purity (carbon content > 95%). No endotoxin was detected, as described previously (Öner et al., 2018a).

2.2. Cell cultures

Human bronchial epithelial cell line (16HBE14o- or 16HBE) was obtained from Dr. Gruenert (University of California, San Francisco). The cell medium was prepared using Dulbecco’s modified eagle medium: nutrient mixture F-1 (DMEM/F12) supplemented with 5% fetal bovine serum (FBS), penicillin (100 U/ml), l-glutamine (2 mM) and fungizone (2.5 μg/ml), purchased from Invitrogen (Merelbeke, Belgium). The cells were cultivated in T25 flasks and incubated at 37 °C in a 100% humidified atmosphere containing 5% CO_2. The cell culture medium was renewed 3 times per week. Approximately 2.5×10^5 cells were sub-cultured in a new cell flask by enzymatically releasing the cells [0.1% trypsin-ethylenediaminetetraacetic acid (EDTA) solution diluted 1/10 in HBSS-]. The cell exposure was initiated when all the cells reached to passage 4.

2.3. Asbestos- and CNT-exposure

The suspension of CNTs was prepared according to the EU project of engineered nanoparticle risk assessment (ENPRA). In brief, CNTs were weighted under HEPA filtered flow using a precision scale. 2.56 mg/ml of CNT concentrations were reached by adding dispersion medium [sterile Baxter water (Versylene, Fresenius, France) containing 2% of FBS]. The solution was sonicated using probe sonication for 16 min. Intermediate concentrations in dispersion medium were prepared prior to the 1/10 diluted final dilutions. 16HBE cells were exposed to 0.25 μg/ml concentration of MWCNTs and SWCNTs in complete cell medium.

Using a precision scale, we weighed amosite (1 mg) in special asbestos-handling cabinets in IDEWE, Belgium. The fibres were dispersed using sterile Baxter water (Versylene, Fresenius, France) consisting 2% of FBS similar to CNTs in order to avoid differences in the epigenetic endpoints. The solutions were sonicated in bath sonication for 10 min in order to create homogenous dilutions. Intermediate concentrations in dispersion medium were prepared prior to final dilutions. Consequently, intermediate dilutions of CNT and asbestos solutions were diluted 1/10 in complete cell culture medium for exposure in order to reach 0.05 μg/ml of exposure. Vehicle suspension was used as a negative control. The suspension was prepared by 1/10 addition of dispersion medium to cell culture medium. A hypomethylating agent, Decitabine (Sigma Aldrich, Brussels, Belgium), was used as a positive control.

Cells were exposed to amosite (0.05 μg/ml), MWCNTs (0.25 μg/ml) and SWCNTs (0.25 μg/ml) 24 h after the cell seeding. Fresh suspensions were prepared prior to each exposure. Cells were exposed in 6-well plate to 5 ml of cell culture media containing the treatment. Therefore, for CNTs (0.25 μg/ml) the equivalent surface area concentration was 0.132 μg/cm^2 and for amosite (0.05 μg/ml) it was 0.026 μg/cm^2. The selection of non-cytotoxic and non-genotoxic doses was based on our previous studies (Ghosh et al., 2017; Gonzalez Guerrico et al., 2005). It may be noted that the selected concentration for sub-chronic exposure was 100-fold lower than the concentrations at which we observed significant epigenetic/transcriptomic alteration for 16 HBE cells in our acute exposure (24 h) study (Ghosh et al., 2018; Öner et al., 2018b, 2018a). Cells were repeatedly exposed every 2–3 days. The spent culture medium was removed, cells were washed with sterile HBSS- to remove unbound fibres, and subsequently refreshed with freshly prepared treatment in cell culture media. The cells from all the exposure conditions were sub-cultured at end of week, and cells were re-seeded at the same density for all conditions.

The exposure protocol was followed for a total of 4 weeks. Airway epithelial cells in vivo have a relatively long turnover rate (Bowden, 1983; Crystal et al., 2008) estimated to be between 30 and 50 days, which may be accelerated by injury. In *in vitro* cell culture however, 16HBE cells have much shorter doubling time (~26 h) and therefore a treatment duration of 4 weeks and recovery of 2 weeks may represent 24–28 and 12–14 doublings respectively. While it is difficult to extrapolate the *in vitro* exposure dose/duration to human working condition, the number of doubling for 4 and 2 weeks may represent 3–4 and 1.5–2 years respectively. The cells harvested at the end of week-4 may therefore be representative of 'sub-chronic exposure' exposure and is referred to as such. After 'sub-chronic exposure' of 4 weeks, cells were cultured for 2 weeks without exposure in complete cell medium. The cells harvested week-6 and are referred to as 'recovery period'. 4 replicates (3 replicates for control) were used for each exposure condition and experiments were repeated two times for epigenetic analyses and cell morphology analysis, respectively.

2.4. Cell number and cytotoxicity

At the end of the exposure weeks, cells were washed and harvested, and the total cell number and the relative cytotoxicity of asbestos and CNTs were measured against the vehicle-treated cells. Cell viability was measured using trypan blue assay.

2.5. Cell morphology and nuclear deposition of CNTs

The cell morphology was analysed in two ways: using light microscopy in cell culture flasks and in cytospin preparations, at 'sub-chronic exposure' and 'recovery period'. For the nuclear deposition study, after three weeks and five weeks, the cells were seeded in 8-well chamber slides. After the cells were attached to the slides, the same exposure protocol was repeated on the chamber slides for one additional week. In this way, the imaging was performed at 'sub-chronic exposure' and 'recovery period' time points. After the exposure period, cells were washed three times using HBSS-, and fixed immediately using 4% paraformaldehyde. Subsequently, the cells were stained using 1/20,000 diluted (in HBSS-) SYBERgold (Invitrogen, Merelbeke, Belgium), and fifty randomly selected cells were scored per exposure as previously described (Öner et al., 2018a). Nuclear deposition of CNTs was investigated using an imaging method developed by Bové et al (Bové et al., 2016). With this method, carbonaceous particles and fibres can be detected inside cellular organelles in a biocompatible and label-free way using femtosecond pulsed laser microscopy. The method has already been validated previously for the detection of CNTs in the cells and more details can be found in our previous publication (Öner et al., 2018a). The technique as previously described, was applied to determine the number of CNT aggregates and the total area of CNTs deposited inside the cells and their corresponding nuclei. Quantitative analysis was done using the image-processing program Fiji (ImageJ v1.47, open source software, http://fiji.sc/Fiji), and was presented as area of aggregates/cell or nucleus in μm^2.

2.6. DNA isolation and microarray

The DNA was isolated using the standard protocol of Qiagen AllPrep DNA/RNA/miRNA Universal kit (QIAGEN, Antwerp, Belgium) at 'sub-chronic exposure' and 'recovery period' time points. DNA quality and quantity were assessed using Nanodrop (Thermo Scientific, 2000c). High quality samples were proceeded for subsequent microarray analysis. DNA (200 ng) was bisulfite-treated using EZ DNA mini kit (Zymo Research, Orange, CA). This allows the conversion of non-methylated cytosine residues to uracil while methylated cytosine residues are not affected. Next, methylation analysis using Infinium MethylationEPIC BeadChip Kit (EPIC) was performed. The microarray provides robust detection of methylation and interrogates over 850 thousand CpG sites (methylation sites) in the whole genome.

2.7. Bioinformatics

The processing of the raw data created by Illumina850K microarray was performed using R software and Bioconductor work packages (Huber et al., 2015). The bioinformatics analyses were performed according to suggested the workflow (Maksimovic et al., 2016). The preprocessing of the data is described briefly as below.

The analyses of the samples collected from 'sub-chronic exposure' and 'recovery period' were conducted separately. The intensity data files in IDAT format were extracted using 'minfi' package (Aryee et al., 2014). Initial quality control was performed and the poor quality probes were deleted. For type I and type II normalisation quantile normalisation method was performed using 'minfi' package (Maksimovic et al., 2012). Further filtering was applied to the probes that have failed in one or more samples.

β values and M values were calculated according to the following formulas, where M represents methylation intensity and U represent unmethylation intensity.

$$\beta = \frac{M}{M + U}$$

$$M = \log_2\left(\frac{\beta}{(1-\beta)}\right)$$

β values were preferred for the description of methylation level of the corresponding probe and M values were preferred for further statistical testing (Du et al., 2010; Zhuang et al., 2012). Further filtering was applied to failed samples.

Batch correction was applied using M values by 'sva' package using combat function (Leek et al., 2012). Next, using a linear model approach and Bayes statistics differentially methylated CpG sites and gene promoter regions were identified. Because of the assay test multiple hypotheses, the p-values were corrected by false discovery rate (FDR). Differential methylation on CpG sites and gene promoter regions provided by Ensemble gene annotation v75 were considered significant when FDR corrected p value (q value) was smaller than 0.05 ($q < 0.05$).

Δβ values are identified according to the following formula:

$$\Delta\beta = \beta\ (exposed) - \beta\ (untreated)$$

Differentially methylated CpG sites and gene promoter regions were annotated to corresponding genes using illumina850K annotation database.

2.8. Statistics

One way ANOVA with Dunnett's comparison was applied for cytotoxicity analysis. Statistical analysis for the microarray was performed as described in section materials and methods bioinformatics. Nuclear deposition measurements were analysed using one-way ANOVA with Tukey's multiple comparison.

3. Results

3.1. Fibre cell interactions

A decrease in total cell number was observed during the treatment period as shown in Fig. 1a, however the changes did not reach statistical significance. The decrease in the cell number was observed for all the treatment groups after 'sub-chronic exposure' period of 4 weeks, which was reverted after a 'recovery period' of two weeks and was comparable to values at the end of Week 1. No cellular toxicity was however noted for MWCNT, SWCNT and amosite after low dose 'sub-chronic exposure' period of 4 weeks and after a 'recovery period' of two weeks (Fig. 1b).

As shown in Fig. 2, no cellular morphology changes were observed. Using light microscopy, we identified that amosite fibres pierced through some cells. MWCNTs and SWCNTs were located inside the cells after the end of 'sub-chronic exposure'. SWCNTs were more present in vesicles and in bigger bundles in comparison to MWCNTs. After the 'recovery period', the fibres/particles were not longer visible under the light microscopy. Growth arrest on the Decitabine-exposed cells was noted even after the 'recovery period'.

Quantitative analysis was performed to measure the number of CNT and the total area of CNT aggregates per cell and nucleus (μm^2) at low dose sub-chronic exposure and after recovery. We used a label-free detection of CNTs using white-light generation under femtosecond pulsed laser illumination. As shown in Fig. 3, both MWCNTs and SWCNTs incorporated in the nuclei after 4 weeks of exposure. The number of CNT aggregates per cell/nucleus, area of CNT aggregates per cell/nucleus as presented in Fig. 3c, showed a significant increase compared to the negative control. The incorporated MWCNT and SWCNT after the sub-chronic exposure were not-detectable after the recovery period. The representative videos were generated (as previously described) from using stained nuclei of the MWCNT- and SWCNT-exposed cells, turning around their axes (see s. 3D-video-MWCNT-chronic and s. 3D-video-SWCNT-chronic).

3.2. Whole genome DNA methylation changes

After low dose MWCNT, SWCNT and amosite 'sub-chronic exposure' and subsequent 'recovery period' time points, the differential methylation was analysed in comparison to their corresponding non-exposed controls using EPIC microarray. The microarray interrogates with more than 850.000 CpG sites and is currently the most comprehensive method to detect DNA methylation across the genome. The differential methylation (either hypomethylation or hypermethylation) was identified when the FDR corrected *p* value was smaller than 0.05 for single CpG site and gene promoter regions. Table 1 shows the number of differential methylation (hypermethylation represented as '+' or hypomethylation represented as '−') of CpG sites and gene promoter regions after exposure to MWCNTs, SWCNTs and amosite. Subsequently, genes were annotated to the differentially methylated probes in order to discuss the possible effect of such DNA methylation changes after each type of exposure.

The differentially methylated CpG sites and gene promoter regions were annotated to genes that they are located on, using illumina850K annotation database. Detailed analysis of the genes and gene functions can be found in Table 2 (the differentially methylated genes after the sub-chronic exposure) and Table 3 (the differentially methylated genes after the recovery). Below, a summary of the results is given and shared genes are reported between CNT- and asbestos-exposed samples.

Negative controls at week 4 (sub-chronic exposure) and week 6 (recovery period), did not show any differential methylation, when compared among each other using the same method.

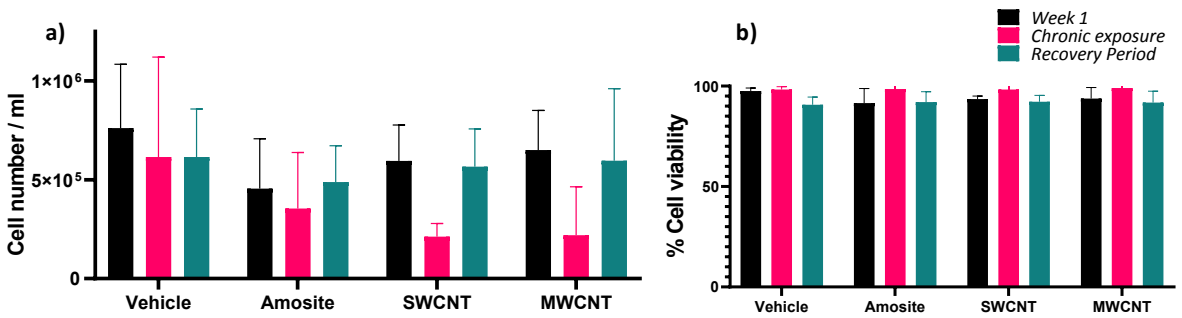

Fig. 1. (a) Cell count and (b) percentage (%) cell viability of the 16HBE cells after the sub-chronic exposure and the recovery period. Trypan blue assay was conducted in order to assess the cellular viability after the low dose 'sub-chronic exposure' to MWCNTs, SWCNTs and amosite and subsequent 'recovery period'. Live cell number/ml and % cell viability were demonstrated on the y-axis, data presented as mean ± SD. No significant decrease in cellular viability was detected using one way ANOVA with Dunnett's multiple comparison.

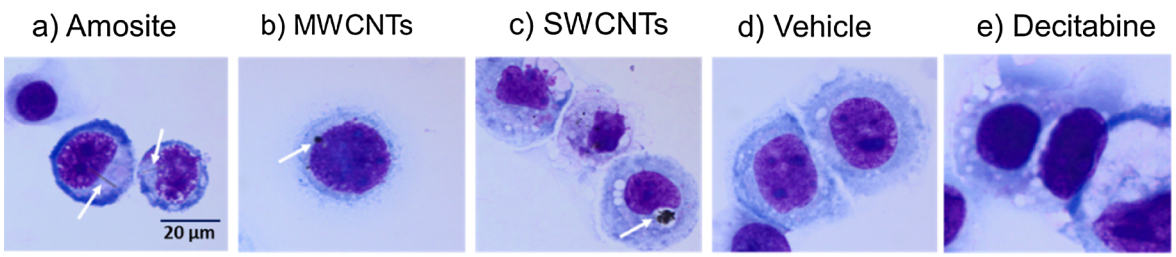

Fig. 2. Images of the 16HBE cells after sub-chronic exposure. The images were taken by light microscopy (Olympus BX61 40x) from cytospin preparations using harvested cells and stained for nucleus. In the images (a) amosite-exposed, (b) MWCNT-exposed, (c) SWCNT-exposed (d) vehicle-exposed and (d) Decitabine-exposed cells were depicted after low dose 'sub-chronic exposure'. The white arrows show asbestos and CNTs in the cell.

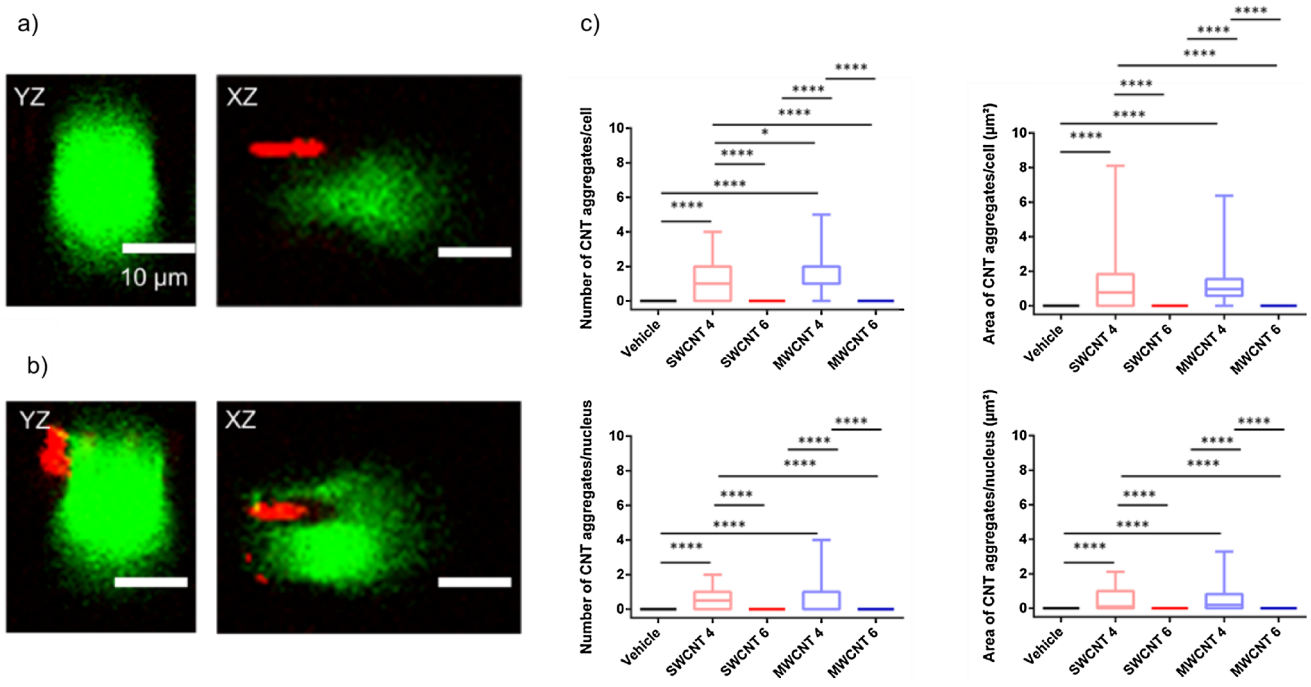

Fig. 3. Nuclear deposition of MWCNTs and SWCNTs in 16HBE cells. The measurement was performed using femtosecond pulsed laser microscopy. (a) Nuclear imaging of MWNCTs. (b) Nuclear imaging of SWCNTs. The nucleus and the CNTs are represented in green and red respectively. Two orthogonal cross sections are shown for each type of CNT. The z-axis is along the optical axis of the microscope. The xy-plane is orthogonal to the z-axis. The scale bar represents 10 µm in each picture. (c) The graphs represent the quantitative analysis of the nuclear deposition of CNTs (number of CNT aggregates per cell, area of CNT aggregates per cell, number of CNT aggregates per nucleus, area of CNT aggregates per nucleus, respectively) after 4 weeks 'sub-chronic exposure' and after the 'recovery period'. The box plots are representing the median, quartiles and 1.5 inter-quartile range of quartiles (whiskers). The statistics were done with one way ANOVA Tukey's multiple comparison (* indicates $p < 0.05$, ** indicates $p < 0.01$, *** indicates $p < 0.001$).

3.2.1. *MWCNTs*

After 'sub-chronic exposure' to MWCNTs, a single CpG site and a single gene promoter were identified to be hypomethylated. The hypomethylated CpG site was located on the Y chromosome. The CpG site was located on thymosin beta 4, Y-linked (*TMSB4Y*) gene, on a promoter associated CpG island. This gene acts in the regulation of actin cytoskeleton and extracellular signal–regulated kinase (ERK) signalling and is known to be deleted in male breast cancer (Wong et al., 2015). The hypomethylated gene promoter located on the RAP1A member of RAS Oncogene Family (*RAP1A)* gene. Activation of this gene might induce aberrant cell proliferation, adhesion, morphological transformation and tumour growth (Zhang et al., 2017). After the 'recovery period', MWCNT-exposed cells did not show any differential methylation compared to control samples either at CpG site or gene promoter region.

3.2.2. *SWCNTs*

Sub-chronic exposure to SWCNTs induced 11 hypermethylated CpG

Table 1
Number of differentially hypermethylation and hypomethylation at CpG site and gene promoter regions after low dose 'sub-chronic exposure' to MWCNTs, SWCNTs and amosite and after the recovery period. The hypermethylated genes were indicated using (+) sign next to the corresponding number. The hypomethylated genes were indicated using (−) sign next to corresponding number.

Fibres	MWCNT		SWCNT		Amosite	
Region of differential methylation	Gene promoter	CpG site	Gene promoter	CpG site	Gene promoter	CpG site
Low dose sub-chronic exposure	1(−)	1(−)	0	11(+)	0	9(+)
After recovery	0	0	0	3(−), 18(+)	0	2(−), 4(+)

Table 2
Differentially methylated functionally meaningful genes after the sub-chronic exposure and their function were listed. The function of the genes were gathered from www.genecards.com. The genes indicated with * were overlapped between amosite and SWCNT-exposed cells. The gene indicated with # was differentially methylated after sub-chronic exposure to SWCNTs and recovery period.

Sub-chronic exposure				
Fibre	Site/region	Gene Name	Gene Symbol	Gene Function
MWCNTs	Gene promoter	RAP1A member of RAS oncogene family	*RAP1A*	Aberrant cell proliferation, adhesion, morphological transformation and tumour growth
	CpG sites	thymosin beta 4, Y-linked	*TMSB4Y*	Regulation of actin cytoskeleton and extracellular signal–regulated kinase (ERK) signalling
SWCNTs	Gene promoter	/NA	/NA	/NA
	CpG sites	ATPase Na + /K + transporting subunit alpha 1 and ATP1A1 antisense RNA 1	*ATP1A1, ATP1A1OS*	Catalytic function for hydrolyses of ATP
		Neurexin	*NRXN3*	Cell adhesion and cell recognition activities
		Chromosome transmission fidelity factor 18	*CHTF18*	Cellular proliferation in particular at the S phase (DNA replication) of the cell cycle
		Glyceraldehyde-3-phosphate dehydrogenase	*GAPDH*	Metabolic function such as glycolysis
		Protease, serine 3	*PRSS3*	Trypsinogen
		Transmembrane protein 123	*TMEM123*	Cell surface receptor and might be involved in cell death
		Hippocalcin Like 1 #	*HPCAL1*	Calcium-binding protein
Amosite	Gene promoter	/NA	/NA	/NA
	CpG sites	NSE2/MMS21 homolog, SMC5-SMC6 complex SUMO ligase	NSMCE2	DNA double-strand break repair pathways
		Matrix metallopeptidase 16	MMP16	Degrading extracellular matrix proteins
		Kruppel like factor 3 *	KLF3	Regulation of the transcription as a sequence-specific DNA binding
		Pituitary tumour-transforming 1 interacting protein	PTTG1IP	Activation of fibroblast growth factor
		RasGEF domain family member 1A	RASGEF1A	Cell migration and cancer related pathways
		Protease, serine 3	PRSS3	Trypsinogen

sites. Eight CpG sites were located on gene regions. After the 'recovery period', 21 differentially methylated CpG sites were identified; three sites were hypomethylated and 18 sites were hypermethylated. Differential methylation on the gene promoter region was not identified.

Comparing the 'sub-chronic exposure' and the 'recovery period', only hypermethylation on HPCAL1 was conserved over the cellular divisions. Furthermore, spontaneous DNA methylation alterations were noted even after the recovery period.

In addition, only hypermethylation on CpG sites was identified after low dose 'sub-chronic exposure' to SWCNT whereas after the 'recovery period', both hypomethylation and hypermethylation were noted.

3.2.3. Amosite

Exposure to amosite induced nine differentially methylated CpG sites. These nine CpG sites were all hypermethylated, similar to

Table 3
Differentially methylated functionally meaningful genes after the recovery period and their function were listed. The function of the genes were gathered from www.genecards.com. The genes indicated with * were overlapped between amosite and SWCNT-exposed cells. The gene indicated with # was differentially methylated after sub-chronic exposure to SWCNTs and recovery period.

Recovery Period				
Fibre	Site/region	Gene Name	Official Gene Symbol	Gene Function
MWCNTs	Gene promoter	/NA	/NA	/NA
	CpG sites	/NA	/NA	/NA
SWCNTs	Gene promoter	/NA	/NA	/NA
	CpG sites	Nuclear transport factor 2 like export factor 1	*NXT1*	Nuclear export factor
		Schlafen-like 1	*SLFNL1*	
		BCL6 corepressor	*BCOR*	Sequence-specific DNA binding and repression of transcription
		Kallikrein related peptidase 3 *	*KLK3*	Serine protease
		ATPase H + transporting V0 subunit D1	*ATP6V0D1*	ATPase
		Kruppel-like factor 3 *	*KLF3*	
		as −1 Homolog C *(EVA1C),*	*EVA1C, FAM176C*	Carbohydrate binding
		Hippocalcin like 1 #	*HPCAL1*	Calcium-binding protein
		POU Class 4 Homeobox 3, RNA binding motif protein 27	*POU4F3*	Sequence-specific DNA binding and transcription regulation.
		RNA binding motif protein 27	*RBM27*	Nucleic acid function activity.
		Inositol polyphosphate phosphatase like 1	*INPPL1*	Insulin function
		EFR3 homolog B	*EFR3B*	Binding function and in regulation of phosphatidylinositol 4-phosphate
Amosite	Gene promoter	/NA	/NA	/NA
	CpG sites	complexin-1	*CPLX1*	Synaptic vesicle exocytosis
		Kallikrein related peptidase 3 *	*KLK3*	Serine protease
		ATPase H + transporting V0 subunit D1	*ATP6V0D1*	ATPase
		Polycomb group ring finger 3	*PCGF3*	Functions to keep the repressive states of group of genes (e.g. HOX group).

SWCNT-exposed cells. Seven CpG sites were located on gene regions. After the 'recovery period', six differentially methylated CpG sites were noted. Two of them were hypomethylated CpG sites and four of them were hypermethylated.

Overall, the epigenetic modifications occurring at 'sub-chronic exposure' were not conserved after the 'recovery period'. However, alterations on CpG sites were noted. Hypermethylation was noted after the sub-chronic exposure but both hypomethylation and hypermethylation were noted after the 'recovery period', similar to SWCNT-exposure.

4. Discussion

CNTs have extremely low density and weight, and therefore can be easily airborne and respirable. During manufacturing and handling, CNTs are found in the air and their adverse effects are being observed in the workers (Fatkhutdinova et al., 2016; Ghosh et al., 2017; Kuijpers et al., 2018; Shvedova et al., 2016; Vlaanderen et al., 2017). CNTs are known to induce lung toxicity via the induction of oxidative stress, inflammation and DNA damage, as evident from previous studies. Exposure to CNTs might directly or indirectly be associated with different diseases including cardiovascular effects, asthma, fibrosis and lung cancer. Epigenetic alterations, including DNA methylation, histone modifications have been widely reported to play a major role in these diseases, especially in the onset and progression of lung cancer. Therefore in our previous studies (Ghosh et al., 2018; Öner et al., 2018a) we wanted to understand the effect of CNT exposure on epigenetic and transcriptomic outcome; and compare them to the changes induced by asbestos (Emerce et al., 2019; Öner et al., 2018b). Since we observed a large number of epigenetic changes in our previous experiments, after acute exposure to CNTs and asbestos, we further wanted to understand the effect and stability of the epigenetic changes after sub-chronic exposure.

At the onset, it would be important to mention that MWCNTs and SWCNTs are not a homogenous group of materials, and therefore mechanistic comparison based on the present study may not be generalized to all CNTs. Therefore, we acknowledge the limitation based on the fact that we have used only one representative material for MWCNT (NM400) and SWCNT (NIST-SRM2483) with different physicochemical properties. However, given the limited existing evidence on CNT induced epigenetic changes, and strong evidence obtained from our previous studies, we believe studying the stability of epigenetic changes at sub-chronic exposure condition and recovery would provide better insight in CNT induced disease onset.

Sub-chronic exposure vs. recovery period: Sub-chronic exposure to MWCNTs revealed accumulation of CNTs in the cells, incorporated around the nuclei. However, only a single CpG site and a gene promoter were hypomethylated. These changes were not present after the recovery period and no significant alterations on other genes were noted. This might mean that hypomethylated CpG sites were recovered or reversed during the recovery period.

Sub-chronic exposure to SWCNTs and amosite, revealed hypermethylation on functionally important genes. After the recovery period without exposure, the differential methylation was still seen. Some of the genes were overlapping between SWCNTs and amosite at different time points ('sub-chronic exposure' and 'recovery period'). These results mean that the differential methylation was not recovered. Interestingly, hypomethylation was seen after the recovery period, which might indicate possible DNA demethylation mechanisms and a repair activity.

Concerning SWCNTs, hippocalcinlike 1 (HPCAL1) gene was differentially methylated after the 'sub-chronic exposure' and the 'recovery period'. The encoded protein of this gene is involved in neuronal calcium-dependent regulation and a member of visinin-family. Visinin-like protein 1 (VILIP1) has been identified as a potential tumour suppressor (Gonzalez Guerrico et al., 2005; Wickborn et al., 2006). In case of hepatocellular carcinoma, HPCAL1 supresses progression by the activation of ERK1/2-MAPK pathway (Zhang et al., 2016). Interestingly one study (Fu et al., 2008) has shown that VILIP1 expression is silenced by epigenetic mechanisms including promoter hypermethylation and histone deacetylation in non-small cell lung cancer (NSCLC) cell lines and primary tumours. Exposure to endocrine disruptors is also know to alters the methylation and transcriptional state of HPCAL1 gene (Tang et al., 2012). Therefore, SWCNT induced CpG hyper methylation in 16 HBE may have functional implication.

SWCNT vs. Amosite: Some genes were differentially methylated after exposure to SWCNTs and amosite at the same or different time points ('sub-chronic exposure' and 'recovery period'). These genes were namely, kruppel-like factor (*KLF3*) and kallikrein related peptidase (*KLK3*).

Two CpG sites that are located on the protease, serine 3 (PRSS3) gene are hypermethylated after the 'sub-chronic exposure' of SWCNTs and amosite exposure. Aberrant alterations on the PRSS3 gene might be particularly important since arsenic exposure-mediated gene promoter methylation was noted in bladder cancer (Marsit et al., 2005). Hypermethylation of KLF3 was noted after the 'sub-chronic exposure' in amosite-exposed cells and after the 'recovery period' in SWCNT-exposed cells. KLF3 gene is associated with the 'transcriptional mis-regulation in cancer' pathway and involved in 'transcription factor activity, sequence-specific DNA binding'. In the literature, Kruppel-like factors are defined as zinc-finger transcription factors and involved in cellular proliferation, differentiation, epithelial-mesenchymal transition (EMT) and metastasis and wide-range of epithelial cancers (Limame et al., 2014; Sachdeva et al., 2015). Hypermethylation of KLK3 gene was noted after the 'recovery period' of amosite and SWCNT-exposed cells. Recent studies highlighted involvement of KLK3 in carcinogenesis, in particular, as a biomarker in prostate cancer (Avgeris et al., 2010; Scorilas and Mavridis, 2014).

It is important to note that we report a small number but potentially very significant genes in our results. This could be due to the very low dose of exposure reflective of real-life conditions. Here, we use very low dose exposure which is at least 40 times or 100 times lower than epigenetic toxicity of CNT found in the literature and from our previous publications (Ghosh et al., 2017; Gulino et al., 2016). The CNTs are insoluble in water suspension and when in the cell medium, particle and medium do not form a homogenous suspension. Therefore, for these very low exposure conditions, the CNTs are not in contact with all the cells. This is also visible from our nuclear deposition assays and cell imaging, where CNTs are in contact with less than 50% of the nuclei. In fact, this can also decrease the observed epigenetic effects, considering only the ones with CNTs in cells alter their epigenetic state. However, these exposures represent the real-time exposure better. Selection of dose and time were specifically adjusted for real-life imitation. For instance, 4 weeks of exposure will potentially imitate an average 3–4 working year of a production worker and 2 weeks will represent duration (1.5–2 years) after cessation of exposure.

Alternatively, performing four replicates might result into limited power in statistical analysis, which might underestimate the significance of the differential methylation. In addition, previous *in vitro* studies show 2–6 replicates are sufficient to create enough power for identification of the differential methylation (Öner et al., 2018a, 2018b, 2017; Sierra et al., 2017). Nevertheless, noted differential alterations are potentially significant and may be associated with an adverse outcome based on the existing literature. Therefore, in our study we emphasize in particular, the potential toxicity of SWCNTs based on noted similarities with the amosite exposure.

5. Authors' statement

DÖ and MG performed the experiments, generated the data and discussed the findings. RC assisted in sections of the data analysis. DÖ prepared the draft manuscript and MG further improved the manuscript

on results and discussion section. HB measured the nuclear uptake of the particles in cells and the nucleus and MA provided the technical assistance for nuclear deposition imaging. MM, pre-processed the DNA methylation and gene expression microarray using bioinformatics techniques and DL was involved in the study design. PH and LG designed, supervised the project and the revised manuscript. PH established the manuscript in final form. All authors read and revised the manuscript and agreed on publication.

Declaration of Competing Interest

The authors declare that they have no known competing financial interests or personal relationships that could have appeared to influence the work reported in this paper.

Acknowledgements

This project was granted by Stichting Tegen Kanker (agreement no: 2012-218, project no: 3M150270). Manosij Ghosh would like to acknowledge Fwo Post-Doctoral Fellowship (12W7718N) and European Respiratory Society RESPIRE Postdoctoral Fellowship (RESPIRE2-2014-7310). Hannelore Bové acknowledges FWO for her post-doctoral fellowship (12P6819N). The authors thank Thomas Van Brussel for the technical assistance.

Appendix A. Supplementary material

Supplementary data to this article can be found online at https://doi.org/10.1016/j.envint.2020.105530.

References

Alshehri, R., Ilyas, A.M., Hasan, A., Arnaout, A., Ahmed, F., Memic, A., 2016. Carbon nanotubes in biomedical applications: factors, mechanisms, and remedies of toxicity. J. Med. Chem. 59, 8149–8167. https://doi.org/10.1021/acs.jmedchem.5b01770.

Aryee, M.J., Jaffe, A.E., Corrada-Bravo, H., Ladd-Acosta, C., Feinberg, A.P., Hansen, K.D., Irizarry, R.A., 2014. Minfi: a flexible and comprehensive Bioconductor package for the analysis of Infinium DNA methylation microarrays. Bioinformatics 30, 1363–1369. https://doi.org/10.1093/bioinformatics/btu049.

Avgeris, M., Mavridis, K., Scorilas, A., 2010. Kallikrein-related peptidase genes as promising biomarkers for prognosis and monitoring of human malignancies. Biol. Chem. 391, 505–511. https://doi.org/10.1515/BC.2010.056.

Bové, H., Steuwe, C., Fron, E., Slenders, E., D'Haen, J., Fujita, Y., Uji-i, H., vandeVen, M., Roeffaers, M., Ameloot, M., 2016. Biocompatible label-free detection of carbon black particles by femtosecond pulsed laser microscopy. Nano Lett. 16, 3173–3178. https://doi.org/10.1021/acs.nanolett.6b00502.

Bowden, D.H., 1983. Cell turnover in the lung. Am. Rev. Respir. Dis. 128. https://doi.org/10.1164/arrd.1983.128.2P2.S46.

Boyles, M.S.P., Young, L., Brown, D.M., MacCalman, L., Cowie, H., Moisala, A., Smail, F., Smith, P.J.W., Proudfoot, L., Windle, A.H., Stone, V., 2015. Multi-walled carbon nanotube induced frustrated phagocytosis, cytotoxicity and pro-inflammatory conditions in macrophages are length dependent and greater than that of asbestos. Toxicol. Vitr. 29, 1513–1528. https://doi.org/10.1016/J.TIV.2015.06.012.

Bussy, C., Pinault, M., Cambedouzou, J., Landry, M.J., Jegou, P., Mayne-L'hermite, M., Launois, P., Boczkowski, J., Lanone, S., 2012. Critical role of surface chemical modifications induced by length shortening on multi-walled carbon nanotubes-induced toxicity. Part. Fibre Toxicol. 9, 46. https://doi.org/10.1186/1743-8977-9-46.

Casalone, E., Allione, A., Viberti, C., Pardini, B., Guarrera, S., Betti, M., Dianzani, I., Aldieri, E., Matullo, G., 2018. DNA methylation profiling of asbestos-treated MeT5A cell line reveals novel pathways implicated in asbestos response. Arch. Toxicol. 92, 1785–1795. https://doi.org/10.1007/s00204-018-2179-y.

Chen, T., Nie, H., Gao, X., Yang, J., Pu, J., Chen, Z., Cui, X., Wang, Y., Wang, H., Jia, G., 2014. Epithelial-mesenchymal transition involved in pulmonary fibrosis induced by multi-walled carbon nanotubes via TGF-beta/Smad signaling pathway. Toxicol. Lett. 226, 150–162. https://doi.org/10.1016/j.toxlet.2014.02.004.

Christensen, B.C., Godleski, J.J., Marsit, C.J., Houseman, E.A., Lopez-Fagundo, C.Y., Longacker, J.L., Bueno, R., Sugarbaker, D.J., Nelson, H.H., Kelsey, K.T., 2008. Asbestos exposure predicts cell cycle control gene promoter methylation in pleural mesothelioma. Carcinogenesis 29, 1555–1559. https://doi.org/10.1093/carcin/bgn059.

Christensen, B.C., Houseman, E.A., Godleski, J.J., Marsit, C.J., Longacker, J.L., Roelofs, C.R., Karagas, M.R., Wrensch, M.R., Yeh, R.-F., Nelson, H.H., Wiemels, J.L., Zheng, S., Wiencke, J.K., Bueno, R., Sugarbaker, D.J., Kelsey, K.T., 2009. Epigenetic profiles distinguish pleural mesothelioma from normal pleura and predict lung asbestos burden and clinical outcome. Cancer Res. 69, 227–234. https://doi.org/10.1158/0008-5472.CAN-08-2586.

Crystal, R.G., Randell, S.H., Engelhardt, J.F., Voynow, J., Sunday, M.E., 2008. Airway epithelial cells: current concepts and challenges. In: Proceedings of the American Thoracic Society, pp. 772–777. https://doi.org/10.1513/pats.200805-041HR.

Donaldson, K., Murphy, F.A., Duffin, R., Poland, C.A., 2010. Asbestos, carbon nanotubes and the pleural mesothelium: a review and the hypothesis regarding the role of long fibre retention in the parietal pleura, inflammation and mesothelioma. Part. Fibre Toxicol. 7, 5. https://doi.org/10.1186/1743-8977-7-5.

Donaldson, K., Poland, C.A., Murphy, F.A., MacFarlane, M., Chernova, T., Schinwald, A., 2013. Pulmonary toxicity of carbon nanotubes and asbestos — Similarities and differences. Adv. Drug Deliv. Rev. 65, 2078–2086. https://doi.org/10.1016/j.addr.2013.07.014.

Du, P., Zhang, X., Huang, C.-C., Jafari, N., Kibbe, W.A., Hou, L., Lin, S.M., 2010. Comparison of Beta-value and M-value methods for quantifying methylation levels by microarray analysis. BMC Bioinf. 11, 587. https://doi.org/10.1186/1471-2105-11-587.

Duke, K.S., Bonner, J.C., 2018. Mechanisms of carbon nanotube-induced pulmonary fibrosis: a physicochemical characteristic perspective. Wiley Interdiscip. Rev. Nanomed. Nanobiotechnol. https://doi.org/10.1002/wnan.1498.

Emerce, E., Ghosh, M., Öner, D., Duca, R.-C., Vanoirbeek, J., Bekaert, B., Hoet, P.H.M., Godderis, L., 2019. Carbon nanotube- and asbestos-induced DNA and RNA methylation changes in bronchial epithelial cells. Chem. Res. Toxicol. https://doi.org/10.1021/acs.chemrestox.8b00406.

Emri, S., Demir, A., Dogan, M., Akay, H., Bozkurt, B., Carbone, M., Baris, I., 2002. Lung diseases due to environmental exposures to erionite and asbestos in Turkey. Toxicol. Lett. 127, 251–257.

Fatkhutdinova, L.M., Khaliullin, T.O., Vasil'yeva, O.L., Zalyalov, R.R., Mustafin, I.G., Kisin, E.R., Birch, M.E., Yanamala, N., Shvedova, A.A., 2016. Fibrosis biomarkers in workers exposed to MWCNTs. Toxicol. Appl. Pharmacol. 299, 125–131. https://doi.org/10.1016/j.taap.2016.02.016.

Fu, J., Fong, K., Bellacosa, A., Ross, E., Apostolou, S., Bassi, D.E., Jin, F., Zhang, J., Cairns, P., de Caceres, I.I., Braunewell, K.H., Klein-Szanto, A.J., 2008. VILIP-1 down-regulation in non-small cell lung carcinomas: Mechanisms and prediction of survival. PLoS One 3. https://doi.org/10.1371/journal.pone.0001698.

Ghosh, M., Öner, D., Duca, R.C., Bekaert, B., Vanoirbeek, J.A., Godderis, L., Hoet, P.H., 2018. Single-walled and multi-walled carbon nanotubes induce sequence-specific epigenetic alterations in 16 HBE cells. Oncotarget 9, 20351–20365. https://doi.org/10.18632/oncotarget.24866.

Ghosh, M., Öner, D., Poels, K., Tabish, A.M., Vlaanderen, J., Pronk, A., Kuijpers, E., Lan, Q., Vermeulen, R., Bekaert, B., Hoet, P.H., Godderis, L., 2017. Changes in DNA methylation induced by multi-walled carbon nanotube exposure in the workplace. Nanotoxicology 1–16. https://doi.org/10.1080/17435390.2017.1406169.

Gonzalez Guerrico, A.M., Jaffer, Z.M., Page, R.E., Braunewell, K.-H., Chernoff, J., Klein-Szanto, A.J., 2005. Visinin-like protein-1 is a potent inhibitor of cell adhesion and migration in squamous carcinoma cells. Oncogene 24, 2307–2316. https://doi.org/10.1038/sj.onc.1208476.

Gulino, G.R., Polimeni, M., Prato, M., Gazzano, E., Kopecka, J., Colombatto, S., Ghigo, D., Aldieri, E., 2016. Effects of chrysotile exposure in human bronchial epithelial cells: Insights into the pathogenic mechanisms of asbestos-related diseases. Environ. Health Perspect. 124, 776–784. https://doi.org/10.1289/ehp.1409627.

Hoet, P.H., Brüske-Hohlfeld, I., Salata, O.V., 2004. Nanoparticles – known and unknown health risks. J. Nanobiotechnol. 2, 12. https://doi.org/10.1186/1477-3155-2-12.

Huber, W., Carey, V.J., Gentleman, R., Anders, S., Carlson, M., Carvalho, B.S., Bravo, H.C., Davis, S., Gatto, L., Girke, T., Gottardo, R., Hahne, F., Hansen, K.D., Irizarry, R.A., Lawrence, M., Love, M.I., MacDonald, J., Obenchain, V., Oleś, A.K., Pagès, H., Reyes, A., Shannon, P., Smyth, G.K., Tenenbaum, D., Waldron, L., Morgan, M., 2015. Orchestrating high-throughput genomic analysis with Bioconductor. Nat. Methods 12, 115–121. https://doi.org/10.1038/nmeth.3252.

Kamp, D.W., 2009. Asbestos-induced lung diseases: an update. Transl. Res. https://doi.org/10.1016/j.trsl.2009.01.004.

Kasai, T., Umeda, Y., Ohnishi, M., Mine, T., Kondo, H., Takeuchi, T., Matsumoto, M., Fukushima, S., 2015. Lung carcinogenicity of inhaled multi-walled carbon nanotube in rats. Part. Fibre Toxicol. 13, 53. https://doi.org/10.1186/s12989-016-0164-2.

Khalil, N., O'Connor, R.N., Flanders, K.C., Unruh, H., 1996. TGF-β1, but Not TGF-β2 or TGF-β3, is differentially present in epithelial cells of advanced pulmonary fibrosis: an immunohistochemical study. Am. J. Respir. Cell Mol. Biol. 14, 131–138. https://doi.org/10.1165/ajrcmb.14.2.8630262.

Kisin, E.R., Murray, A.R., Keane, M.J., Shi, X.-C., Schwegler-Berry, D., Gorelik, O., Arepalli, S., Castranova, V., Wallace, W.E., Kagan, V.E., Shvedova, A.A., 2007. Single-walled carbon nanotubes: geno- and cytotoxic effects in lung fibroblast V79 cells. J. Toxicol. Environ. Heal. Part A 70, 2071–2079. https://doi.org/10.1080/15287390701601251.

Kuijpers, E., Pronk, A., Kleemann, R., Vlaanderen, J., Lan, Q., Rothman, N., Silverman, D., Hoet, P., Godderis, L., Vermeulen, R., 2018. Cardiovascular effects among workers exposed to multiwalled carbon nanotubes. Occup. Environ. Med. https://doi.org/10.1136/oemed-2017-104796.

Leek, J.T., Johnson, W.E., Parker, H.S., Jaffe, A.E., Storey, J.D., 2012. The sva package for removing batch effects and other unwanted variation in high-throughput experiments. Bioinformatics 28, 882–883. https://doi.org/10.1093/bioinformatics/bts034.

Limame, R., de Beeck, K.O., Lardon, F., De Wever, O., Pauwels, P., 2014. Krüppel-like factors in cancer progression: three fingers on the steering wheel. Oncotarget 5, 29–48. https://doi.org/10.18632/oncotarget.1456.

Maksimovic, J., Gordon, L., Oshlack, A., 2012. SWAN: Subset-quantile Within Array Normalization for Illumina Infinium HumanMethylation450 BeadChips. Genome Biol. 13, R44. https://doi.org/10.1186/gb-2012-13-6-r44.

Maksimovic, J., Phipson, B., Oshlack, A., 2017. A cross-package bioconductor workflow for analysing methylation array data. F1000Research 5, 1281. https://doi.org/10.

12688/f1000research.8839.3.
Marsit, C.J., Karagas, M.R., Danaee, H., Liu, M., Andrew, A., Schned, A., Nelson, H.H., Kelsey, K.T., 2005. Carcinogen exposure and gene promoter hypermethylation in bladder cancer. Carcinogenesis 27, 112–116. https://doi.org/10.1093/carcin/bgi172.
Muller, J., Delos, M., Panin, N., Rabolli, V., Huaux, F., Lison, D., 2009. Absence of carcinogenic response to multiwall carbon nanotubes in a 2-year bioassay in the peritoneal cavity of the rat. Toxicol. Sci. 110, 442–448. https://doi.org/10.1093/toxsci/kfp100.
Murphy, F.A., Poland, C.A., Duffin, R., Al-Jamal, K.T., Ali-Boucetta, H., Nunes, A., Byrne, F., Prina-Mello, A., Volkov, Y., Li, S., Mather, S.J., Bianco, A., Prato, M., MacNee, W., Wallace, W.A., Kostarelos, K., Donaldson, K., 2011. Length-dependent retention of carbon nanotubes in the pleural space of mice initiates sustained inflammation and progressive fibrosis on the parietal pleura. Am. J. Pathol. 178, 2587–2600. https://doi.org/10.1016/J.AJPATH.2011.02.040.
Norbet, C., Joseph, A., Rossi, S.S., Bhalla, S., Gutierrez, F.R., 2015. Asbestos-related lung disease: a pictorial review. Curr. Probl. Diagn. Radiol. 44, 371–382. https://doi.org/10.1067/j.cpradiol.2014.10.002.
Öner, D., Ghosh, M., Bové, H., Moisse, M., Boeckx, B., Duca, R.C., Poels, K., Luyts, K., Putzeys, E., Van Landuydt, K., Vanoirbeek, J.A., Ameloot, M., Lambrechts, D., Godderis, L., Hoet, P.H., 2018a. Differences in MWCNT- and SWCNT-induced DNA methylation alterations in association with the nuclear deposition. Part. Fibre Toxicol. 15, 11. https://doi.org/10.1186/s12989-018-0244-6.
Öner, D., Ghosh, M., Moisse, M., Duca, R.C., Coorens, R., Vanoirbeek, J.A.J., Lambrechts, D., Godderis, L., Hoet, P.H.M., 2018b. Global and gene-specific DNA methylation effects of different asbestos fibres on human bronchial epithelial cells. Environ. Int. 115, 301–311. https://doi.org/10.1016/j.envint.2018.03.031.
Öner, D., Moisse, M., Ghosh, M., Duca, R.C., Poels, K., Luyts, K., Putzeys, E., Cokic, S.M., Van Landuyt, K., Vanoirbeek, J., Lambrechts, D., Godderis, L., Hoet, P.H., 2017. Epigenetic effects of carbon nanotubes in human monocytic cells. Mutagenesis 32. https://doi.org/10.1093/mutage/gew053.
Poland, C.A., Duffin, R., Kinloch, I., Maynard, A., Wallace, W.A.H., Seaton, A., Stone, V., Brown, S., MacNee, W., Donaldson, K., 2008. Carbon nanotubes introduced into the abdominal cavity of mice show asbestos-like pathogenicity in a pilot study. Nat. Nanotechnol. 3, 423–428. https://doi.org/10.1038/nnano.2008.111.
Polimeni, M., Gulino, G.R., Gazzano, E., Kopecka, J., Marucco, A., Fenoglio, I., Cesano, F., Campagnolo, L., Magrini, A., Pietroiusti, A., Ghigo, D., Aldieri, E., 2016. Multi-walled carbon nanotubes directly induce epithelial-mesenchymal transition in human bronchial epithelial cells via the TGF-β-mediated Akt/GSK-3β/SNAIL-1 signalling pathway. Part. Fibre Toxicol. 13, 27. https://doi.org/10.1186/s12989-016-0138-4.
Poulsen, S.S., Jackson, P., Kling, K., Knudsen, K.B., Skaug, V., Kyjovska, Z.O., Thomsen, B.L., Clausen, P.A., Atluri, R., Berthing, T., Bengtson, S., Wolff, H., Jensen, K.A., Wallin, H., Vogel, U., 2016. Multi-walled carbon nanotube physicochemical properties predict pulmonary inflammation and genotoxicity. Nanotoxicology 10, 1263–1275. https://doi.org/10.1080/17435390.2016.1202351.
Rasmussen, K., Mast, J., De Temmerman, P.-J., Verleysen, E., Waegeneers, N., Van Steen, F., Christophe Pizzolon, J., De Temmerman, L., Van Doren, E., Alstrup Jensen, K., Birkedal, R., Axel Clausen, P., Kembouche, Y., Thieriet, N., Spalla, O., Guiot, C., Rousset, D., Witschger, O., Bau, S., Bianchi, B., Shivachev, B., Dimowa, L., Nikolova, R., Nihtianova, D., Tarassov, M., Petrov, O., Bakardjieva, S., Motzkus, C., Labarraque, G., Oster, C., Cotogno, G., Gailliard, C., 2013. JRC Reposit.: NM-Ser. Represent. Manuf. Nanomater. https://doi.org/10.2788/10753.
Sachdeva, M., Dodd, R.D., Huang, Z., Grenier, C., Ma, Y., Lev, D.C., Cardona, D.M., Murphy, S.K., Kirsch, D.G., 2015. Epigenetic silencing of Kruppel like factor-3 increases expression of pro-metastatic miR-182. Cancer Lett. 369, 202–211. https://doi.org/10.1016/j.canlet.2015.08.016.
Sargent, L.M., Hubbs, A.F., Young, S.-H., Kashon, M.L., Dinu, C.Z., Salisbury, J.L., Benkovic, S.A., Lowry, D.T., Murray, A.R., Kisin, E.R., Siegrist, K.J., Battelli, L., Mastovich, J., Sturgeon, J.L., Bunker, K.L., Shvedova, A.A., Reynolds, S.H., 2012. Single-walled carbon nanotube-induced mitotic disruption. Mutat. Res. Toxicol. Environ. Mutagen. 745, 28–37. https://doi.org/10.1016/j.mrgentox.2011.11.017.
Sargent, L.M., Porter, D.W., Staska, L.M., Hubbs, A.F., Lowry, D.T., Battelli, L., Siegrist, K.J., Kashon, M.L., Mercer, R.R., Bauer, A.K., Chen, B.T., Salisbury, J.L., Frazer, D., McKinney, W., Andrew, M., Tsuruoka, S., Endo, M., Fluharty, K.L., Castranova, V., Reynolds, S.H., 2014. Promotion of lung adenocarcinoma following inhalation exposure to multi-walled carbon nanotubes. Part. Fibre Toxicol. 11, 3. https://doi.org/10.1186/1743-8977-11-3.
Scorilas, A., Mavridis, K., 2014. Predictions for the future of kallikrein-related peptidases in molecular diagnostics. Expert Rev. Mol. Diagn. 14, 713–722. https://doi.org/10.1586/14737159.2014.928207.
Selikoff, I.J., Hammond, E.C., Seidman, H., 1980. Latency of asbestos disease among insulation workers in the United States and Canada. Cancer 46, 2736–2740.
Shvedova, A.A., Kisin, E., Murray, A.R., Johnson, V.J., Gorelik, O., Arepalli, S., Hubbs, A.F., Mercer, R.R., Keohavong, P., Sussman, N., Jin, J., Yin, J., Stone, S., Chen, B.T., Deye, G., Maynard, A., Castranova, V., Baron, P.A., Kagan, V.E., 2008. Inhalation vs. aspiration of single-walled carbon nanotubes in C57BL/6 mice: inflammation, fibrosis, oxidative stress, and mutagenesis. Am. J. Physiol. Cell. Mol. Physiol. 295, L552–L565. https://doi.org/10.1152/ajplung.90287.2008.
Shvedova, A.A., Yanamala, N., Kisin, E.R., Khailullin, T.O., Birch, M.E., Fatkhutdinova, L.M., Nurkiewicz, T., 2016. Integrated analysis of dysregulated ncRNA and mRNA expression profiles in humans exposed to carbon nanotubes. PLoS One 11, e0150628. https://doi.org/10.1371/journal.pone.0150628.
Sierra, M.I., Rubio, L., Bayón, G.F., Cobo, I., Menendez, P., Morales, P., Mangas, C., Urdinguio, R.G., Lopez, V., Valdes, A., Vales, G., Marcos, R., Torrecillas, R., Fernández, A.F., Fraga, M.F., 2017. DNA methylation changes in human lung epithelia cells exposed to multi-walled carbon nanotubes. Nanotoxicology 11, 857–870. https://doi.org/10.1080/17435390.2017.1371350.
Tabish, A.M., Poels, K., Byun, H.-M., Luyts, K., Baccarelli, A.A., Martens, J., Kerkhofs, S., Seys, S., Hoet, P., Godderis, L., 2017. Changes in DNA methylation in mouse lungs after a single intra-tracheal administration of nanomaterials. PLoS One 12. https://doi.org/10.1371/journal.pone.0169886.
Tang, W., Morey, L.M., Cheung, Y.Y., Birch, L., Prins, G.S., Ho, S., 2012. Neonatal exposure to Estradiol/Bisphenol A alters promoter methylation and expression of *Nsbp1* and *Hpcal1* genes and transcriptional programs of *Dnmt3a/b* and *Mbd2/4* in the ratprostate gland throughout life. Endocrinology 153, 42–55. https://doi.org/10.1210/en.2011-1308.
Timbrell, V., Rendall, R.E.G., 1972. Preparation of the UICC Standard reference samples of asbestos. Powder Technol. 5, 279–287. https://doi.org/10.1016/0032-5910(72)80032-9.
Vlaanderen, J., Pronk, A., Rothman, N., Hildesheim, A., Silverman, D., Hosgood, H.D., Spaan, S., Kuijpers, E., Godderis, L., Hoet, P., Lan, Q., Vermeulen, R., 2017. A cross-sectional study of changes in markers of immunological effects and lung health due to exposure to multi-walled carbon nanotubes. Nanotoxicology 11, 395–404. https://doi.org/10.1080/17435390.2017.1308031.
Wickborn, C., Klein-Szanto, A.J., Schlag, P.M., Braunewell, K.-H., 2006. Correlation of-visinin-like-protein-1 expression with clinicopathological features in squamous cell carcinoma of the esophagus. Mol. Carcinog. 45, 572–581. https://doi.org/10.1002/mc.20201.
Wong, H.Y., Wang, G.M., Croessmann, S., Zabransky, D.J., Chu, D., Garay, J.P., Cidado, J., Cochran, R.L., Beaver, J.A., Aggarwal, A., Liu, M.-L., Argani, P., Meeker, A., Hurley, P.J., Lauring, J., Park, B.H., 2015. TMSB4Y is a candidate tumor suppressor on the Y chromosome and is deleted in male breast cancer. Oncotarget 6, 44927–44940. https://doi.org/10.18632/oncotarget.6743.
Zhang, Y., Liu, Y., Duan, J., Yan, H., Zhang, J., Zhang, H., Fan, Q., Luo, F., Yan, G., Qiao, K., Liu, J., 2016. Hippocalcin-like 1 suppresses hepatocellular carcinoma progression by promoting p21(Waf/Cip1) stabilization by activating the ERK1/2-MAPK pathway. Hepatology 63, 880–897. https://doi.org/10.1002/hep.28395.
Zhang, Y.L., Wang, R.C., Cheng, K., Ring, B.Z., Su, L., 2017. Roles of Rap1 signaling in tumor cell migration and invasion. Cancer Biol. Med. https://doi.org/10.20892/j.issn.2095-3941.2016.0086.
Zhuang, J.J., Widschwendter, M., Teschendorff, A.E., 2012. A comparison of feature selection and classification methods in DNA methylation studies using the Illumina Infinium platform. BMC Bioinf. 13, 59. https://doi.org/10.1186/1471-2105-13-59.